GPR Imaging of a Fracture Zone in the Vaucluse Karst Aquifer Using 2D and 3D Eikonal Inversion

Daryl Van Vorst[1] (darylv@ece.ubc.ca), Matthew Yedlin[1] (matty@ece.ubc.ca),
Yves Guglielmi[2] (yves.guglielmi@univ-provence.fr), Frédéric Cappa[3] (cappa@geoazur.unice.fr),
Stéphane Gaffet[3] (gaffet@geoazur.unice.fr), Michael Maxwell[4] (Michael_Maxwell@golder.com),
Doug Oldenburg[1] (doug@eos.ubc.ca)

1. *University of British Columbia, Vancouver, BC, Canada*
2. *Géologie des Systèmes Carbonatés, Universite de Provence Aix-Marseille, Marseille, France*
3. *Géosciences Azur, UNS/CNRS/OCA, Valbonne, France*
4. *Golder Associates, Burnaby, BC, Canada*

Keywords*: Inversion, eikonal, travel time, ray, 3D*

ABSTRACT

An efficient and easily implemented 2D and 3D travel-time inversion algorithm is present and applied to data collected within a karst aquifer. The results provide an indication of water content, and are consistent with known site features.

INTRODUCTION

This work focuses on the application of 2D and 3D travel-time inversion codes to cross-borehole GPR data collected from the karst aquifer at LSBB (Laboratoire Souterrain à Bas Bruit), near Rustrel, France. The use of a simple and efficient fast sweeping solver for the eikonal equation makes this code fast and easy to implement (using a combination of C and GNU Octave). The 3D portion of this work is an extension of the previous 2D implementation [1].

FORMULATION

The inversion is formulated in the typical way as a least squares minimization problem [2] defined by:

$$\begin{aligned}\phi &= \phi_d + \beta\phi_m \\ &= \left\| W_d\left(F[m] - d^{obs}\right)\right\|^2 + \\ &\qquad \beta\sum_{n=1}^{N}\alpha_n\left\|W_n\left(m - m_{ref}\right)\right\|^2\end{aligned} \tag{1}$$

In (1), ϕ_d and ϕ_m are a measure of data misfit and model smoothness, respectively. $F[m]$ represents the forward modeling operation that depends on the model parameters (slowness), m. The measured data, d^{obs}, are the travel times from transmitter to receiver (as determined by picking the time-domain GPR traces). W_d is a matrix that allows the incorporation of both differences in measurement uncertainty for each data point and correlation of measurement errors. In this work, it is a diagonal matrix with elements that are the reciprocal of the associated data point's estimated standard deviation. Here, the matrices W_n are derivatives in the two or three coordinate directions and the α_n terms are set to unity (N = 2 or 3, depending on the dimensionality of the problem). Additional or different model constraints can be built in by changing the W_n matrices, or adding more of them. The regularization parameter, β, is manually chosen such that a reasonable compromise is made between data fitting and model smoothness.

EIKONAL EQUATION

In the high frequency limit, Maxwell's equations can be simplified to the eikonal equation,

$$\left|\nabla\tau(\mathbf{r})\right| = \frac{1}{v(\mathbf{r})} = s(\mathbf{r}), \tag{2}$$

where $\tau(\mathbf{r})$ is the travel time of a ray from the source location to any other location within the domain, and $s(\mathbf{r})$ is the model slowness ($v(\mathbf{r})$ is the velocity). An efficient, robust, and easy to implement fast sweeping solver [3] is used to solve (2).

Once the travel time from source to any point within the model is known, rays can be traced from receiver back to source by following the gradient of the travel time (this is much simpler than traditional ray tracing). The length of the ray path in each cell is used as an approximation of the true sensitivity ($d\tau(\mathbf{r}_{rx})/ds(\mathbf{r})$), which is used to iteratively minimize (1).

DATA PICKING

In order to use the raw time-domain GPR data for travel-time inversion, it is necessary to pick the arrival times. This was accomplished by finding the correlation peak between a pre-determined approximation of a typical GPR waveform and the data. A heuristic algorithm was applied that first estimates where in each gather (which receiver position) there is the cleanest signal. From this point, the algorithm follows that arrival through the gather by finding the correlation peak within a small window (in time) centered at the previously determined pick. This results in the rejection later or earlier arrivals.

The rejection of later arrivals is desired because the employed eikonal forward modeling code only determines the first arrival time. When both the transmitting and receiving antennas are near the surface, prior arrivals to the "best" one (at least within the collected data set) are due to the GPR signal traveling through the air. Rejecting this arrival allows us to restrict the modeling domain to the subsurface region. An obvious benefit of this is an increase in computation efficiency due to a smaller domain. Additionally, it is likely that the inversion is more accurate because the second arrival has traveled through the near-surface material and thus contains additional data to aid in reconstruction of the near-surface region. It is nearly equivalent to a first arrival if the domain had been bounded by a continuation of the earth, rather than by air.

MEASUREMENTS

Measurements were taken using a MALÅ Geoscience 250 MHz borehole radar system in 5 boreholes, arranged as shown in Fig. 1. For hole pairs 1-5, 5-2, and 3-4, the transmitter was held at five regularly spaced depths within the boreholes and receiver measurements were made at 5 cm intvervals (not all of the receiver data was used for these inversions). For hole pairs 5-3, 5-4, 2-3, 2-4, the transmitter was held at three regularly spaced intervals.

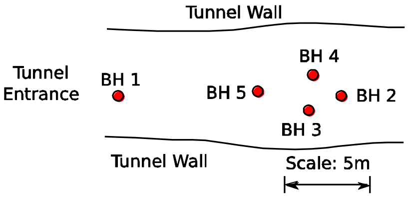

Fig. 1 Layout of the measurement area within the anti-blast gallery at LSBB. Only hole positions are to scale.

INVERSION RESULTS

2D tomograms (Fig. 2) were produced for the hole pairs 1-5, 5-2, and 3-4. The volume of interest for the 3D inversion is around the cluster of four holes to the right. No radar measurements were taken between holes 1 and 4 or holes 1 and 3, so there is no substantial data to support 3D inversion in the volume to the left of hole 5.

The 3D inversion results are shown below in Fig. 3, and a televiewer image taken from borehole 2 is shown for comparison. It is immediately clear that the inversion matches the televiewer image from a purely structural point of view. The high-porosity region that is visible in the middle of the televiewer image lines up with a high permittivity region in the inverted data (in both the 2D and 3D cases). In order for this to be consistent, the high-porosity region must have high water content, otherwise that region should have lower permittivity than the surrounding rock. This is consistent with the very wet conditions found in the tunnel and that the high porosity zone is highly fractured.

The regularization parameter that was chosen for the 3D inversion was selected in favour of better data fitting (and added structure). Some inversion artifacts are readily seen (such as distortion near the boreholes where there is a very high concentration of ray paths).

CONCLUSION

The results of 2D and 3D eikonal-based inversions have been presented, and are shown to be consistent with the borehole televiewer data.

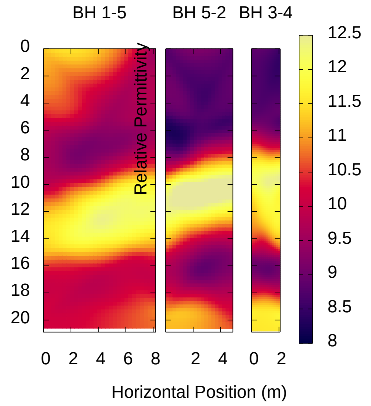

Fig. 2 Recovered relative permittivity using the 2D algorithm.

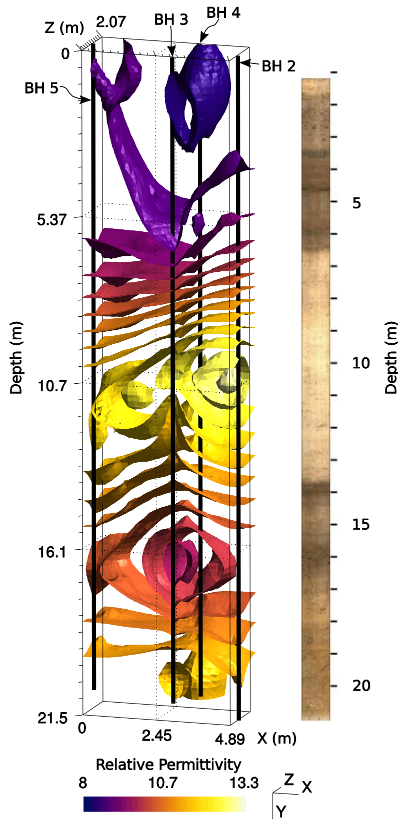

Fig. 3 Recovered electric relative permittivity using the 3D inversion algorithm (left) and televiewer image for borehole 2 (right). The light-colored region in the televiewer image (between 6.5 to 13.5m) is a low-porosity region. Fifteen isosurfaces at regular intervals from 8 to 13.3 are shown.

REFERENCES

[1] M. Yedlin, D. Van Vorst, Y. Guglielmi, F. Cappa, & S. Gaffet, *AGU 2009 Fall Meeting*, Poster NS31A-1152.

[2] D. Aldridge & D. Oldenburg, *J. Seis. Expl.*, **2** (1993), 257-274.

[3] H. Zhao, *J. Math. Comp.*, **74** (2004), 603-627.